J. Fluid Mech. (1997), *vol.* 340, *pp.* 319–341. Printed in the United Kingdom

Velocity distribution function for a dilute granular material in shear flow

By V. KUMARAN

Department of Chemical Engineering, Indian Institute of Science, Bangalore 560 012, India

(Received 18 February 1996 and in revised form 15 December 1996)

The velocity distribution function for the steady shear flow of disks (in two dimensions) and spheres (in three dimensions) in a channel is determined in the limit where the frequency of particle–wall collisions is large compared to particle–particle collisions. An asymptotic analysis is used in the small parameter ϵ, which is naL in two dimensions and na^2L in three dimensions, where n is the number density of particles (per unit area in two dimensions and per unit volume in three dimensions), L is the separation of the walls of the channel and a is the particle diameter. The particle–wall collisions are inelastic, and are described by simple relations which involve coefficients of restitution e_t and e_n in the tangential and normal directions, and both elastic and inelastic binary collisions between particles are considered. In the absence of binary collisions between particles, it is found that the particle velocities converge to two constant values $(u_x, u_y) = (\pm V, 0)$ after repeated collisions with the wall, where u_x and u_y are the velocities tangential and normal to the wall, $V = (1 - e_t)V_w/(1 + e_t)$, and V_w and $-V_w$ are the tangential velocities of the walls of the channel. The effect of binary collisions is included using a self-consistent calculation, and the distribution function is determined using the condition that the net collisional flux of particles at any point in velocity space is zero at steady state. Certain approximations are made regarding the velocities of particles undergoing binary collisions in order to obtain analytical results for the distribution function, and these approximations are justified analytically by showing that the error incurred decreases proportional to $\epsilon^{1/2}$ in the limit $\epsilon \to 0$. A numerical calculation of the mean square of the difference between the exact flux and the approximate flux confirms that the error decreases proportional to $\epsilon^{1/2}$ in the limit $\epsilon \to 0$. The moments of the velocity distribution function are evaluated, and it is found that $\langle u_x^2 \rangle \to V^2$, $\langle u_y^2 \rangle \sim V^2\epsilon$ and $-\langle u_x u_y \rangle \sim V^2\epsilon \log(\epsilon^{-1})$ in the limit $\epsilon \to 0$. It is found that the distribution function and the scaling laws for the velocity moments are similar for both two- and three-dimensional systems.

1. Introduction

Rapid shear flows of granular materials are encountered in many situations such as rock slides, snow avalanches, and in numerous industrial applications involving the transport of solids. Rapid flows involve widely spaced particles in vigorous motion, where the transport of momentum and energy is due to instantaneous particle–wall and particle–particle collisions. This is in contrast to slow deformations, where there is extended contact between particles and the transport of momentum and energy occurs due to tangential and normal frictional forces. In rapid shear flows, the particle motion is driven by the motion of the walls, and momentum and energy are

transported by particle collisions with the wall and with other particles. For such flows, it is natural to exploit the analogy between the motion of the particles and the motion of molecules in an ideal gas, and to seek a description similar to the kinetic theory for gases. Such a description is difficult, however, due to the nonlinear nature of the Boltzmann equation for the particles. In an ideal gas of elastic particles at equilibrium, it is possible to use the Boltzmann H-Theorem to show that the velocity distribution function is a Gaussian (Maxwell–Boltzmann) distribution. For systems near equilibrium, an asymptotic scheme, the Enskog expansion (Chapman & Cowling 1970), can be used with the Maxwell–Boltzmann distribution as the leading approximation. Most of the previous analyses of shear flows have used the Maxwell–Boltzmann distribution as the starting point, but this approximation is valid when the coefficient of elasticity is close to 1, the time between successive collisions is small compared to the inverse of the strain rate and the distance between the walls is large compared to the mean free path of the particles (low-Knudsen-number limit). However, an approximation of this type cannot be used in the opposite limit, where the coefficient or restitution may not be close to 1, and the distance travelled by a particle between successive binary collisions is large compared to the distance between the walls (high-Knudsen-number limit). The objective of the present study is to use asymptotic analysis to determine the distribution function in the high Knudsen number limit where the coefficient of restitution may not be close to 1.

The analogy between the motion of particles in rapid shear and that of molecules in a gas has been used to develop kinetic theories for the rapid flow of granular materials (Jenkins & Savage 1983; Lun *et al.* 1984; Jenkins & Richman 1988; for a review see Jenkins 1987). In these models, there is a granular 'temperature' associated with the random fluctuating motion of the particles, and in addition to the mass and momentum equations, it is necessary to write a conservation equation for the temperature. Constitutive equations that take into account both frictional and collisional transport of momentum have been proposed by Savage (1982) and Johnson & Jackson (1987). Another issue of importance in the study of granular flows is the form of the boundary conditions, in particular the boundary condition for the granular temperature at the bounding surfaces. Jenkins & Richman (1986) obtained the boundary conditions from microscopic models for the interaction between the particle and the wall due to a specific geometric structure of the wall. Johnson & Jackson (1987) have used a more simple specularity condition, and included both frictional and kinetic transport effects in their boundary conditions. Recently, Jenkins & Askari (1991) have considered the interface between particles that are sheared and particles that are stationary on average, and treated the boundary using methods similar to that of Jenkins & Richman (1986).

The form of the constitutive equation for the temperature is considered to be similar to the heat equation in the Chapman–Enskog theory of dense gases (Chapman & Cowling 1970), and the dependence of the viscosity and thermal conductivity on the temperature is assumed to be of the same form as that for a dense gas. In using these equations it is explicitly or implicitly assumed that the velocity distribution function of the particles is close to the Maxwell–Boltzmann distribution for a gas at equilibrium. However, in practical situations the distribution function could be very different due to many reasons. The Maxwell–Boltzmann distribution is valid only for elastic particles, while in practice most granular flows involve inelastic particles. Even for slightly inelastic particles when the coefficient of elasticity is close to 1, the Maxwell–Boltzmann distribution can only be used when the time between successive collisions is small compared to the inverse of the strain rate, and when the mean free path is

small compared to the width of the channel. In view of the restrictive regime where the Maxwell–Boltzmann equation is applicable, it is necessary to examine other methods of deriving the particle distribution function in order to model realistic physical situations. However, this is complicated due to the nonlinear nature of the Boltzmann equation, and a general class of solutions is not available. In the present study, asymptotic analysis is used to derive the distribution function in the limit opposite to the Maxwell–Boltzmann limit, i.e. in the limit where the coefficient of elasticity may not be close to 1, and the particle–wall collisions are more frequent compared to particle–particle collisions. Since the calculation of the distribution function explicitly includes the details of the particle–particle and particle–wall collisions, it is not necessary to make any assumptions regarding the form of the boundary conditions once the model for the particle dynamics is identified.

A distribution function that is very different from the Maxwell–Boltzmann distribution was derived earlier by Kumaran & Koch (1993) for a bidisperse suspension of particle settling in a gas. In this case, particles collisions due to a difference in the terminal velocities of the two species induce fluctuations, and the drag force due to the gas reduces the fluctuations and brings the particle velocities back to their terminal velocities. In the limit where the viscous relaxation time of the particles is small compared to the time between collisions, most of the particles have velocities close to their terminal velocities, while there are a few particles which have velocities very different from their terminal velocities soon after a collision. An asymptotic analysis was used to examine this limit, and the distribution functions are delta functions at the terminal velocities of the two species in the absence of binary collisions in the leading approximation. The effect of binary collisions between particles travelling at their terminal velocities on the distribution function was determined using a perturbation analysis in the small parameter τ_v/τ_c, where τ_v is the viscous relaxation time and τ_c is the time between successive collisions. It was found that the distribution function diverges near the terminal velocities of the two species, and is non-zero in a finite region in velocity space. The moments of the distribution function were calculated, and these were in agreement with the simulation results of Kumaran, Tsao & Koch (1993) with no adjustable parameters. Tsao and Koch (1995) extended this to the shear flow of a dilute monodisperse suspension of particles in a gas. Here, collisions are induced between particles travelling along streamlines with different velocities whose separation is less than a particle diameter, and the viscous dissipation in the gas tends to bring the particles back to the velocity of the streamline along which they are travelling.

In the present study, a similar analysis is carried out for the shear flow of a granular material between two plates. The number density of the particles n is low enough that the parameter $\epsilon = nLa^2$ is small, where L is the distance between the plates and a is the particle diameter. Note that ϵ, the ratio of the distance between the plates and the distance between successive binary collisions, is the inverse of the Knudsen number (Cercignani 1975). In this case, particle–wall collisions are more frequent than particle–particle collisions, and the particle–wall collisions transfer momentum to the particles in the tangential direction. In order to model this transfer, the particle–wall collisions are considered to be inelastic with constant coefficients of restitution in the tangential and normal directions. The binary collisions between the particles are considered to be elastic in most of the analysis, but the effect of inelastic collisions is also considered. The particle transport in velocity space due to wall and binary collisions is determined, and the distribution function at steady state is calculated by equating the fluxes into and out of a differential volume in velocity space. The

moments of the distribution function are then calculated. The analysis is developed for inelastic disks in a two-dimensional geometry in the next section, since the transport of particles in velocity space is more easily visualized in two dimensions. The extension to inelastic spheres in three dimensions is briefly discussed in §3.

2. Inelastic disks in two dimensions

In the present section, the velocity distribution function for a two-dimensional set of disks sheared between two plane surfaces is analysed in the limit where the frequency of wall collisions is large compared to that of binary collisions between the disks. The configuration consists of a channel of width L and infinite length containing disks of diameter a with number density n per unit area, with the origin of the coordinate system located at the centre of the channel. The walls of the channel move with velocities V_w and $-V_w$, and the tangential force exerted by the wall on the particles causes particle motion. If the particle velocities in the x- and y-directions are of the same magnitude, the frequency of wall collisions is small compared to that of binary collisions for $naL \ll 1$. The particle–wall collisions are inelastic, and the coefficient of restitution is e_n for the normal velocity and e_t for the tangential velocity, where e_t and e_n are both less than 1. The components of the velocity of a particle after a wall collision, (u'_x, u'_y), are related to the components before the collision, (u_x, u_y), as follows:

$$u'_x = e_t u_x \pm (1 - e_t)V_w, \quad u'_y = -e_n u_y. \tag{2.1}$$

In the equation for u'_x, the positive sign for V_w is used for collisions with the wall at $y = L/2$, and the negative sign for collisions with the wall at $y = -L/2$. In (2.1), the equation for the change in the tangential velocity u_x states that the post collisional relative velocity between the particle and wall is e_t times the precollisional relative velocity. Equations similar to (2.1) have been used often in previous studies, for example in Jenkins & Richman (1985), Lun & Savage (1987) and Lun (1991). The coefficients of restitution are not constants in general, and could depend on the inelasticity, the particle surface friction coefficient and the impact velocity. The effect of a normal-velocity-dependent coefficient of restitution was considered by Lun & Savage (1987), who assumed that e_n was an exponentially increasing function of the normal velocity. More complex collision laws which incorporate normal and tangential coefficients of restitution and tangential friction have been formulated by Walton (1992) and used by Jenkins (1992), and these have been verified experimentally by Foerster *et al.* (1994). However, the computations become quite complex even for this simple form of the friction coefficient. In the present analysis, as in the studies of Jenkins & Richman (1985) and Lun (1991), the coefficients of restitution are assumed to be constants to simplify the calculations. The binary collisions between particles are considered to be elastic in most of the analysis, but the effect of inelastic binary collisions on the velocity distribution function is briefly discussed at the end of this section.

The derivation of the distribution function is a self-consistent derivation, and the steady state distribution function is derived by equating the fluxes of particles into and out of a differential volume in velocity space. However, before presenting the self-consistent analysis, it is useful to discuss the physical mechanism for the generation of particle velocity fluctuations in the flow. A collision of a particle with the wall has two effects. The first is to decrease the velocity of the particle normal to the wall, thereby dampening the fluctuations normal to the wall. The second is to alter the tangential

velocity by an amount proportional to the difference between the particle velocity and the wall velocity, thereby increasing the velocity fluctuations in this direction. If we consider an initial state where the particles have some velocity fluctuations in the y-direction and neglect binary collisions, the effect of repeated collisions with the walls would tend to reduce the normal velocity to zero, while the tangential velocity would converge to a set of velocities which are regenerated after successive collisions with the two walls of the channel. This final velocity can be obtained by considering two successive collisions of the particle, first with the wall at $y = L/2$ and second with the wall at $y = -L/2$. After the first collision, the particle velocity in the x-direction is

$$u_x' = e_t u_x + (1 - e_t)V_w, \tag{2.2}$$

and the velocity after the second collision is

$$\begin{aligned} u_x'' &= e_t u_x' - (1 - e_t)V_w \\ &= e_t^2 u_x - (1 - e_t)^2 V_w. \end{aligned} \tag{2.3}$$

If the tangential velocity of the particle is recovered after two successive collisions, $u_x'' = u_x$, and the velocity of the particle is

$$\left.\begin{aligned} u_x = -V &= \frac{-(1 - e_t)V_w}{1 + e_t}, \\ u_x' = V &= \frac{(1 - e_t)V_w}{1 + e_t}. \end{aligned}\right\} \tag{2.4}$$

If the initial distribution of particle velocities in the y-direction is symmetric about $u_y = 0$, the distribution function in the final state would consist of an equal number of particles with velocities at $(\pm V, 0)$, with small fluctuations about these velocities. The velocity after i collisions with the walls of a particle with initial velocity $(u_x^{(0)}, u_y^{(0)})$ is

$$u_x + (-1)^i(1 + (-1)^{(i-1)}e_t^i)V = e_t^i u_x^{(0)}, \quad u_y = (-1)^i e_n^i u_y^{(0)}, \tag{2.5}$$

where it is assumed that the first collision takes place with the wall at $y = +L/2$. A symmetrical argument applies if the first collision takes place with the wall at $y = -L/2$.

In deriving the above trajectory of the particles, the effect of binary collisions has been neglected. However, binary collisions are important when the velocity u_y becomes small. The frequency of wall collisions (per unit area) is proportional to nu_y/L, while the frequency of binary collisions (per unit area) is proportional to $n^2 aV$. The frequency of wall collisions is of the same magnitude as that of binary collisions for $u_y \sim \epsilon V$, or $e_n^i \sim \epsilon$. In this case, it is necessary to take into account the effect of binary collisions in a small region of radius ϵV about the points $(\pm V, 0)$. The binary collisions cause a dispersion in the particle velocities, and produce the y-component of the velocity required for wall collisions. The wall collisions then tend to reduce the particle velocities back to the values $(\pm V, 0)$. Consequently, at steady state, most of the particles have velocities near $(\pm V, 0)$, while a relatively small number of particles have velocities $O(V)$ different from $(\pm V, 0)$. For particles with velocities near $(\pm V, 0)$, the dominant mechanism of dispersion is binary collisions, since the velocity of these particles normal to the wall is small, while for particles with velocities $O(V)$ different from $(\pm V, 0)$, the dominant mechanism of dispersion is particle–wall collisions, which tend to reduce the velocity of these

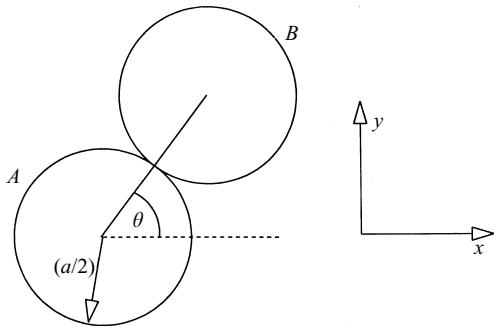

FIGURE 1. The coordinate system for analysing the binary collision between two disks in the two-dimensional geometry.

particles to $(\pm V, 0)$. The qualitative picture presented here is formalized using a self-consistent derivation of the distribution function at steady state in the following analysis.

The distribution function is derived self-consistently using an asymptotic expansion in the small parameter $\epsilon = naL$. The effect of binary collisions on the dispersion of particle velocities is considered first. As indicated earlier, transport in velocity space due to binary collisions is large compared to that due to particle–wall collisions when the particles velocities are close to $(\pm V, 0)$. Therefore, while calculating the flux due to binary collisions correct to leading order in small ϵ, it is assumed that the colliding particles have velocities $(\pm V, 0)$. It will be shown a little later that at steady state, the root-mean-square fluctuating velocity of the particles in the y-direction is $O(\epsilon^{1/2}V)$ and the root mean square of the deviation of the velocities in the x-direction from $\pm V$ is $O(\epsilon^{1/2}V)$. Consequently, it is expected that the error incurred in the post-collisional velocities due to the assumption that the precollisional velocities are $(\pm V, 0)$ decreases proportional to $\epsilon^{1/2}V$ in the asymptotic limit $\epsilon \to 0$. In addition, the error in the collisional fluxes due to the assumption regarding the precollisional velocities is verified in another manner later in the analysis. The collisional fluxes are calculated using the approximate distribution function in two ways. In the first, the flux is estimated using the actual precollisional velocities of the two particles, and in the second the precollisional velocities are assumed to be $(\pm V, 0)$. The mean square of the difference in the fluxes evaluated in these two ways is computed and integrated over velocity space. It is observed that the root mean square of the difference in the fluxes does decrease proportional to $\epsilon^{1/2}$ in the limit $\epsilon \to 0$, thereby justifying the above qualitative arguments.

Consider a collision between particle A with velocity $(u_{Ax}, u_{Ay}) = (V, 0)$ and particle B with velocity $(u_{Bx}, u_{By}) = (-V, 0)$. The result of the collision depends on the angle made by the line joining the centres of the particles at the point of contact with the direction of the relative velocity, θ, as shown in figure 1. The components of the velocity after the collision are

$$\left.\begin{aligned} u'_{Ax} &= -V\cos(2\theta), \quad u'_{Ay} = -V\sin(2\theta), \\ u'_{Bx} &= V\cos(2\theta), \qquad u'_{By} = V\sin(2\theta). \end{aligned}\right\} \tag{2.6}$$

If the components of the velocity are expressed in polar coordinates in velocity space,

the final velocities of the two particles are

$$\left.\begin{aligned} u_A &= V, \quad \chi_A = \pi + 2\theta, \\ u_B &= V, \quad \chi_B = 2\theta, \end{aligned}\right\} \tag{2.7}$$

where u_A and u_B are the distances from the origin in velocity space, and χ_A and χ_B are the polar angles. In the above equations, χ_A varies between 0 and 2π, while χ_B varies between $-\pi$ and π. Equation (2.7) indicates that binary collisions transport particles onto a circle of radius V centred at the origin in velocity space, and there is an accumulation of particles on this circle due to binary collisions. There is a depletion of particles because of the change in velocity due to wall collisions, and the density of particles on this circle is determined by a balance between these two, as shown below.

The frequency of collisions between particles per unit area in which the angle between the line of centres and the relative velocity is in the range $\mathrm{d}\theta$ about θ is

$$\text{Frequency / Area} = (n/2)^2(2V)a\cos(\theta)\mathrm{d}\theta. \tag{2.8}$$

Using the relation between χ_A, χ_B and θ (2.7), the following relations can be obtained for the collisional influx of particles (per unit area) in the differential angle $\mathrm{d}\chi_A$ about χ_A and $\mathrm{d}\chi_B$ about χ_B on the circle of radius V in velocity space:

$$\left.\begin{aligned} N_A^{in}(\chi_A)\mathrm{d}\chi_A &= \tfrac{1}{4}n^2Va\left[\cos\left(\tfrac{1}{2}\chi_A - \tfrac{1}{2}\pi\right)\right]\mathrm{d}\chi_A, \\ N_B^{in}(\chi_B)\mathrm{d}\chi_B &= \tfrac{1}{4}n^2Va\left[\cos\left(\tfrac{1}{2}\chi_B\right)\right]\mathrm{d}\chi_B. \end{aligned}\right\} \tag{2.9}$$

Here, the indices A and B refer to the particles that have a precollisional x-velocity in the positive and negative directions respectively. The collisional fluxes for particles of type A and B are written separately because the ranges of the angles χ_A and χ_B are different: χ_A varies between 0 and 2π, while χ_B varies between $-\pi$ and π. At steady state, there is a flux of particles out of the circle of radius V due to particle collisions with the wall. This flux (per unit area) is

$$N_I^{out}(\chi_I)\mathrm{d}\chi_I = (n|u_{Iy}|/L)f_{I0}(\chi_I)\mathrm{d}\chi_I \tag{2.10}$$

for $I = A$ and $I = B$. Here, $f_{I0}(\chi_I)$ is the distribution function along the circle of radius V in velocity space after the binary collision, and $nf_{I0}(\chi_I)d\chi_I$ is the number of particles per unit area in the differential angle $\mathrm{d}\chi_I$ about χ_I. At steady state, $N_I^{out} = N_I^{in}$, and f_{I0} is

$$\left.\begin{aligned} f_{A0}(\chi_A) &= \frac{\epsilon}{4|\sin(\chi_A)|}\left[\cos\left(\tfrac{1}{2}\chi_A - \tfrac{1}{2}\pi\right)\right], \\ f_{B0}(\chi_B) &= \frac{\epsilon}{4|\sin(\chi_B)|}\left[\cos\left(\tfrac{1}{2}\chi_B\right)\right]. \end{aligned}\right\} \tag{2.11}$$

The above distribution function diverges near $\chi_A = \pi$ and $\chi_B = 0$. This is because at these points, the velocity u_y is zero, and there is no depletion of particles due to wall collisions. However, it is necessary to take into account the depletion due to binary collisions at these points, since they are of the same magnitude as the wall collisions. The modified flux of particles (per unit volume) is

$$N_I^{out}(\chi_I)\mathrm{d}\chi_I = (n|u_y|/L + 2n^2aV)f_{I0}(\chi_I)\mathrm{d}\chi_I. \tag{2.12}$$

In deriving the above expression, we have assumed that the velocities of the colliding particles are $(V, 0)$ and $(-V, 0)$. This approximation is correct to $O(\epsilon^{1/2})$ for particles

with $u_y \sim O(\epsilon^{1/2}V)$. For particles with $u_y \sim O(V)$, there is an $O(1)$ error in the estimation of the frequency of the binary collisions. However, for these particles, the depletion of particles due to binary collisions is $O(\epsilon)$ smaller than that due to wall collisions, and so the error made in the estimate of the total flux is $O(\epsilon)$ in this region. Therefore, the above expression for the particle flux is in error by a maximum of $O(\epsilon^{1/2})$. The error incurred due to this approximation is evaluated quantitatively later on in the present section. A measure of the error $\langle E^2 \rangle$ is defined as the integral over the velocity space of the square of the difference between the 'exact flux' evaluated using the approximate distribution function and the exact velocity difference between the particles, and the approximate flux evaluated using the approximate distribution function and setting the velocity difference equal to $(2V, 0)$. It is observed that the square root of this error does decrease proportional to $\epsilon^{1/2}$, as anticipated by the qualitative arguments used here.

The modified distribution functions, determined by incorporating the approximate expression for the collisional flux, (2.12), are

$$\left.\begin{aligned} f_{A0}(\chi_A) &= \frac{\epsilon}{4(|\sin(\chi_A)| + 2\epsilon)} \left[\cos\left(\tfrac{1}{2}\chi_A - \tfrac{1}{2}\pi\right)\right], \\ f_{B0}(\chi_B) &= \frac{\epsilon}{4(|\sin(\chi_B)| + 2\epsilon)} \left[\cos\left(\tfrac{1}{2}\chi_B\right)\right]. \end{aligned}\right\} \tag{2.13}$$

The particles with velocity distribution function $f_{I0}(\chi_I)$ (for $I = A$ and B) subsequently undergo collisions with the wall, and their velocities after i collisions are given in (2.5). From (2.5) (and the symmetrical equation for the case where the first collision is with the wall at $-L/2$), it can be inferred that the particles which have undergone i collisions with the wall after the most recent binary collision are located on contours in velocity space

$$\left.\begin{aligned} u_{Ix}^{(i)} + (1 + (-1)^{(i-1)}e_t^i)V &= e_t^i V \cos(\chi_I) \quad \text{for} \quad 0 < \chi_I < \pi, \\ u_{Ix}^{(i)} - (1 + (-1)^{(i-1)}e_t^i)V &= e_t^i V \cos(\chi_I) \quad \text{for} \quad \pi < \chi_I < 2\pi, -\pi < \chi_I < 0, \\ u_{Iy}^{(i)} &= e_n^i V \sin(\chi_I). \end{aligned}\right\} \tag{2.14}$$

The above equations show that the particle positions are located along ellipses C_i centred at $(\pm(1+(-1)^{(i-1)}e_t^i)V, 0)$ with radii $e_t^i V$ and $e_n^i V$ along the x- and y-directions. The contours C_i for $e_n = 0.7$ and $e_t = 0.7$ are shown in figure 2.

The distribution function along each of these contours at steady state can be obtained by a flux balance in velocity space as before. The rate of accumulation of particles on the contour C_i, due to collisions between the particles on the contour C_{i-1} and the wall, is

$$N_{Ii}^{in} \mathrm{d}\chi_I = (n|u_{Iy}^{(i-1)}|/L) f_{I(i-1)}(\chi_I) \mathrm{d}\chi_I. \tag{2.15}$$

The rate of depletion of particles on the contour C_i, due to collisions of particles on this contour with the wall, is

$$N_{Ii}^{out} \mathrm{d}\chi_I = (n|u_{Iy}^{(i)}|/L) f_{Ii}(\chi_I) \mathrm{d}\chi_I. \tag{2.16}$$

In addition, it is necessary to include the depletion of particles due to binary collisions for the reasons discussed above when calculating $f_{I0}(\chi_I)$. When calculating this depletion for a particle on contour C_i, it is assumed that the difference in the velocities of the two particles is $(2V, 0)$. This is correct to $O(\epsilon^{1/2})$ when the velocities of the colliding particles are $O(\epsilon^{1/2}V)$ different from $(\pm V, 0)$. When the particle velocities

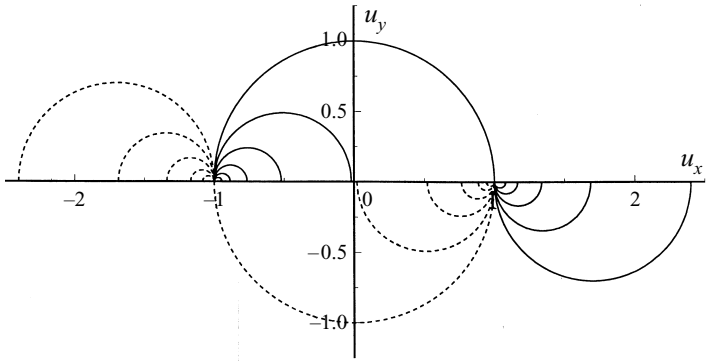

FIGURE 2. The contours C_i of the particle velocities in the (u_x, u_y)-plane, where the index i represents the number of times the particle has collided with the walls after its most recent binary collision. The solid lines show the location of particles whose first collision is with the wall at $y = +L/2$, while the broken lines show the location of particles whose first collision is with the wall at $y = -L/2$. The coefficients of restitution e_t and e_n are both 0.7.

are $O(V)$ different from $(\pm V, 0)$, the error made due to this approximation is $O(1)$. However, in this case, the flux due to binary collisions is $O(\epsilon)$ smaller than that due to wall collisions, and the error made in the estimate of the total flux is $O(\epsilon)$. Therefore, the above approximation has a maximum error of $O(\epsilon^{1/2})$ throughout velocity space. Equation (2.16), modified to include the depletion due to binary collisions, is

$$N_{Ii}^{out} \mathrm{d}\chi_I = \left[n|u_{Iy}^{(i)}|/L + 2n^2 aV \right] f_{Ii}(\chi_I) \mathrm{d}\chi_I. \tag{2.17}$$

Equating N_{Ii}^{in} and N_{Ii}^{out} at steady state, we get

$$f_{Ii}(\chi_I) = \frac{f_{I(i-1)}(\chi_I)}{e_n} \left[1 + \frac{2\epsilon V}{|u_{Iy}^{(i)}|} \right]^{-1}, \tag{2.18}$$

where $u_y^{(i)} = e_n^i V \sin(\chi_I)$. The distribution function $f_{Ii}(\chi_I)$ can be expressed in terms of $f_{I0}(\chi_I)$ by induction:

$$f_{Ii}(\chi_I) = \frac{f_{I0}(\chi_I)}{e_n^i} \prod_{j=1}^{i} \left[1 + \frac{2\epsilon}{(e_n)^j |\sin(\chi_I)|} \right]^{-1}. \tag{2.19}$$

This provides the final distribution function for the particle distribution along the contours C_i in velocity space. It is difficult to analytically simplify the above expression further. However, it can easily be verified that the above distribution function is normalized, i.e.

$$\sum_{i=0}^{\infty} \left[\int_0^{2\pi} \mathrm{d}\chi_A f_{Ai}(\chi_A) + \int_{-\pi}^{\pi} \mathrm{d}\chi_B f_{Bi}(\chi_B) \right] = 1. \tag{2.20}$$

The relation

$$\sum_{1}^{\infty} e_n^{-i} \prod_{j=1}^{i} \left[1 + \frac{2\epsilon}{e_n^j |\sin(\chi)|} \right]^{-1} = \frac{|\sin(\chi)|}{2\epsilon} \tag{2.21}$$

is useful for deriving the normalization condition (2.20). The identity (2.21) is proved by expanding the left-hand side in a Taylor series in the variable e_n.

The qualitative features of the distribution function are as follows. As i increases,

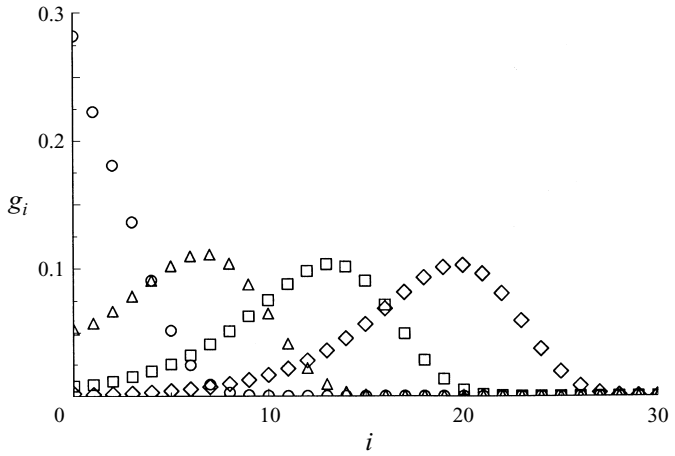

FIGURE 3. The number of particles g_i on contour C_i as a function of i. The coefficients of restitution e_t and e_n are both 0.7. ◯, $\epsilon = 10^{-1}$; △, $\epsilon = 10^{-2}$; □, $\epsilon = 10^{-3}$; ◇, $\epsilon = 10^{-4}$.

the distribution function increases as e_n^{-i} till $e_n^i \sim \epsilon$. This is because the frequency of wall collisions decreases as u_y decreases. However, as i is further decreased, there is a decrease in the distribution function proportional to $\epsilon^{-1}e_n^{i(i-1)}$, because the effect of binary collisions becomes significant in this region. The function

$$g_i = \int_0^{2\pi} \mathrm{d}\chi_A f_{Ai}(\chi_A) + \int_{-\pi}^{\pi} \mathrm{d}\chi_B f_{Bi}(\chi_B) \tag{2.22}$$

is shown as a function of the index i for $e_n = 0.7$ and $\epsilon = 10^{-1}, 10^{-2}, 10^{-3}$ and 10^{-4} in figure 3. This figure shows that the number of particles along the contour C_i decreases with an increase in i for $\epsilon = 0.1$, indicating that the approximation made in deriving the particle flux due to binary collisions is not valid for this case. However, there is an increase and then a decrease in g_i, as anticipated above, for ϵ between 10^{-2} and 10^{-4}, and the value of i at which g_i is a maximum increases as $-\log(\epsilon)$. Figure 4 shows the number of particles g_i as a function of u_i, which is the radius of the semicircle which forms contour C_i, and is a measure of the deviation in the velocity of particles along C_i from the closer of $(\pm V, 0)$. This figure shows that the deviation from $(\pm V, 0)$ is large for $\epsilon = 10^{-1}$, but most particles have velocities close to $(\pm V, 0)$ for $\epsilon \leqslant 10^{-2}$, as anticipated in the asymptotic analysis. The position of the maximum of g_i varies as $u_i = e_n^{-\log(\epsilon)}$.

It is useful to estimate the magnitude of the errors incurred while calculating the distribution function. While calculating the collisional fluxes $N_{Ii}^{in}(\chi_I)$ and $N_{Ii}^{out}(\chi_I)$, approximate expressions were used for the flux due to binary collisions. The actual errors incurred while evaluating the fluxes cannot be determined since the exact expression for the distribution function is not known. However, it is possible to estimate the error made in the fluxes using the present asymptotic expression for the distribution function. If the error made is small, it can be inferred that the asymptotic distribution function is close to the exact distribution function. In the evaluation of $N_{Ii}^{out}(\chi)$, only particles with velocities close to $(\pm V, 0)$ were considered, and the velocity difference between the two colliding particles was approximated as $2V$. The 'exact

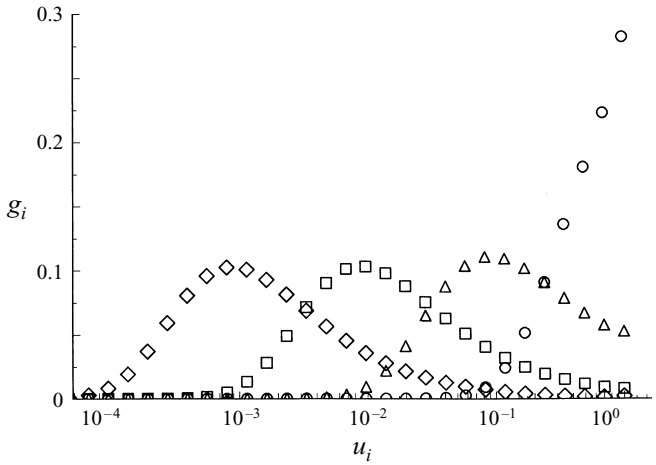

FIGURE 4. The number of particles g_i on contour C_i as a function u_i, the radius of contour C_i. The coefficients of restitution e_t and e_n are both 0.7. ○, $\epsilon = 10^{-1}$; △, $\epsilon = 10^{-2}$; □, $\epsilon = 10^{-3}$; ◇, $\epsilon = 10^{-4}$.

relation' for $\mathcal{N}_{out}(\chi)$ is

$$\mathcal{N}_{Ii}^{out}(\chi_I) = (nu_{Iy}^{(i)}/L) f_{Ii}(\chi_I) + 2n^2 a \sum_{J=A,B} \sum_{j=0}^{\infty} \int \mathrm{d}\chi_J f_{Ii}(\chi_I) f_{Jj}(\chi_J) |\boldsymbol{u}_I^{(i)} - \boldsymbol{u}_J^{(j)}|, \qquad (2.23)$$

where the limits of integration of χ_J are 0 to 2π if $J = A$, and $-\pi$ to π if $J = B$. In the above expression, the second term on the right is the frequency of binary collisions calculated using the exact velocity difference between the particles and the approximate distribution function. The difference between the above exact expression and the approximate expression (2.12) is due to the approximation made in treating binary collisions:

$$[\mathcal{N}_{Ii}^{out}(\chi_I) - N_{Ii}^{out}(\chi_I)] = 2n^2 a f_{Ii}(\chi_I) \left[\left(\sum_{J=A,B} \sum_{j=0}^{\infty} \int \mathrm{d}\chi_J f_{Jj}(\chi_J) |\boldsymbol{u}_I^{(i)} - \boldsymbol{u}_J^{(j)}| \right) - V \right]. \qquad (2.24)$$

An estimate of the square of the magnitude of the total error incurred can be obtained by integrating the square of the quantity in the square brackets in (2.24) over all values of χ and summing it over all i as follows:

$$\langle E^2 \rangle = \sum_{I=A,B} \sum_{i=0}^{\infty} \int \mathrm{d}\chi_I f_{Ii}(\chi_I) \left[\left(\sum_{J=A,B} \sum_{j=0}^{\infty} \int \mathrm{d}\chi_J f_{Jj}(\chi_J) \left(\frac{|\boldsymbol{u}_I^{(i)} - \boldsymbol{u}_j^{(j)}|}{V} \right) \right) - 1 \right]^2. \qquad (2.25)$$

The root-mean-square error $\langle E^2 \rangle^{1/2}$ is shown as a function of ϵ for different values of the coefficient of restitution in figure 5. It can be seen that in the limit $\epsilon \to 0$, the root mean square of the error in the fluxes is proportional to $\epsilon^{1/2}$, as anticipated while deriving the fluxes. This validates the previous assumption that the expressions for the fluxes are correct to $O(\epsilon^{1/2})$ in the limit $\epsilon \to 0$.

The moments of the velocity distribution function can now be evaluated using (2.19) and (2.13):

$$\langle \psi(\boldsymbol{u}) \rangle = \sum_{i=0}^{\infty} \left[\int_0^{2\pi} \mathrm{d}\chi_A \psi(\boldsymbol{u}_A^{(i)}) f_{Ai}(\chi_A) + \int_{-\pi}^{\pi} \mathrm{d}\chi_B \psi(\boldsymbol{u}_B^{(i)}) f_{Bi}(\chi_B) \right], \qquad (2.26)$$

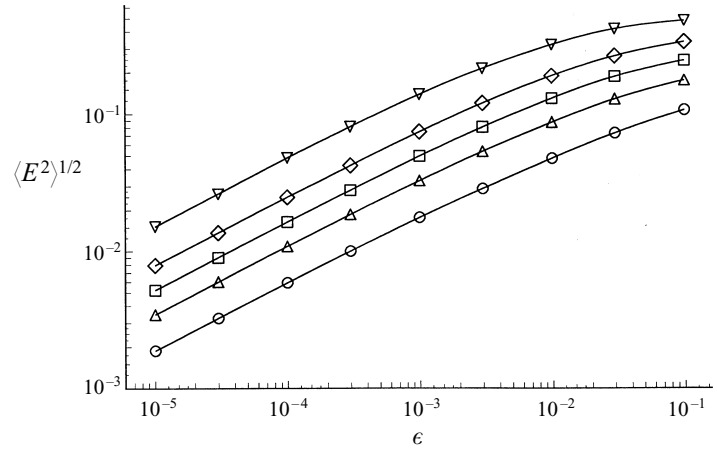

FIGURE 5. The root mean square of the error, $\langle E^2\rangle^{1/2}$ as a function of ϵ for ◯, $e_t = e_n = 0.1$; △, $e_t = e_n = 0.3$; □, $e_t = e_n = 0.5$; ◇, $e_t = e_n = 0.7$; ∇, $e_t = e_n = 0.9$.

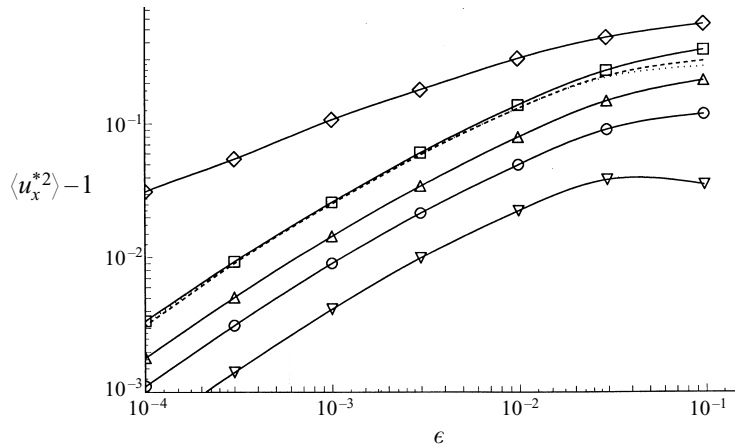

FIGURE 6. The mean-square velocity $\langle u_x^{*2}\rangle - 1$ as a function of ϵ. ◯, $e_t = e_n = 0.3, e = 1.0$; △, $e_t = e_n = 0.5, e = 1.0$; □, $e_t = e_n = 0.7, e = 1.0$; ◇, $e_t = 0.3, e_n = 0.7, e = 1.0$; ∇, $e_t = 0.3, e_n = 0.7, e = 1.0$; – – – –, $e_t = e_n = 0.7, e = 0.7$; · · · · · ·, $e_t = e_n = 0.7, e = 0.5$.

where $\psi(\boldsymbol{u})$ is a function of the particle velocities. It is necessary to evaluate the sum and integral in (2.26) numerically, and in the numerical calculations the upper limit of the index i was chosen large enough that a variation of 10 in i changed the value of the moment by less than 10^{-6} times the value of the moment. The integral over the angle χ was evaluated using Simpson's rule, and the step size chosen was 10^{-3}. Using this scheme, then error in the normalization condition (2.20) ($\psi(\boldsymbol{u}) = 1$) was less than 10^{-6} for all the results discussed here.

The results shown here are for the scaled velocity moments $\psi(\boldsymbol{u}^*)$, where $\boldsymbol{u}^* = (\boldsymbol{u}/V)$ and $V = (1 - e_t)V_w/(1 + e_t)$. The moments of the velocity distribution function have the following behaviour in the limit $\epsilon \to 0$.

(*a*) The mean-square velocity $\langle u_x^{*2}\rangle$ tends to a constant value $\langle u_x^{*2}\rangle = 1$ since the particle velocities in the x-direction asymptotically approach $\pm V$. The deviation of the mean-square velocity from ± 1, $\langle u_x^{*2}\rangle - 1$, is shown as a function of ϵ for different values of the coefficient of restitution in figure 6. The deviation has the asymptotic

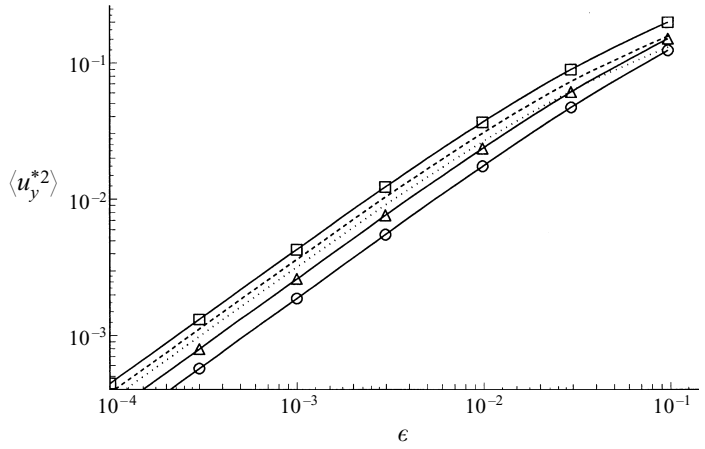

FIGURE 7. The mean-square velocity $\langle u_y^{*2}\rangle$ as a function of ϵ. ◯, $e_n = 0.3, e = 1.0$; △, $e_n = 0.5, e = 1.0$; □, $e_n = 0.7, e = 1.0$; — — ——, $e_n = 0.7, e = 0.7$; ·····, $e_n = 0.7, e = 0.5$.

behaviour

$$\lim_{\epsilon\to 0}\left(\langle u_x^{*2}\rangle - 1\right) \sim \epsilon^{\beta} \quad \text{for } e_t^2 > e_n$$
$$\sim \epsilon \quad \text{for } e_t^2 < e_n, \tag{2.27}$$

where $0 < \beta < 1$.

(*b*) Figure 7 shows $\langle u_y^{*2}\rangle$ as a function of ϵ and e_n. Note that $\langle u_y^{*2}\rangle$ is only a function of e_n and is independent of e_t. From figure 7, it can easily be seen that

$$\lim_{\epsilon\to 0}\langle u_y^{*2}\rangle \sim \epsilon. \tag{2.28}$$

(*c*) The cross-correlation, $-\langle u_x^* u_y^*\rangle$, is shown as a function of ϵ for different values of the coefficient of restitution in figure 8. The behaviour of this function is

$$\lim_{\epsilon\to 0}\left(-\langle u_x^* u_y^*\rangle\right) \sim -\epsilon\log(\epsilon). \tag{2.29}$$

The above asymptotic expressions can be derived using relations similar to (2.21) for the infinite sum in the expression for the distribution function. In particular, the following three relations are useful for obtaining the asymptotic behaviour:

$$\lim_{\epsilon\to 0}\sum_{1}^{\infty}\prod_{j=1}^{i}\left[1+\frac{2\epsilon}{e_n^j|\sin(\chi)|}\right]^{-1} \sim \log(\epsilon), \tag{2.30}$$

$$\lim_{\epsilon\to 0}\sum_{1}^{\infty}(-1)^{(i-1)}p^i\prod_{j=1}^{i}\left[1+\frac{2\epsilon}{e_n^j|\sin(\chi)|}\right]^{-1} \to \text{constant}, \tag{2.31}$$

$$\lim_{\epsilon\to 0}\sum_{1}^{\infty}p^i\prod_{j=1}^{i}\left[1+\frac{2\epsilon}{e_n^j|\sin(\chi)|}\right]^{-1} \sim \epsilon^{-\alpha} \quad \text{for } p > 1$$
$$\to \text{constant} \quad \text{for } p < 1. \tag{2.32}$$

Here, p is a constant and the exponent α is a function of p and e_n, and varies between 0 and 1. The above results are difficult to derive analytically, and were obtained using

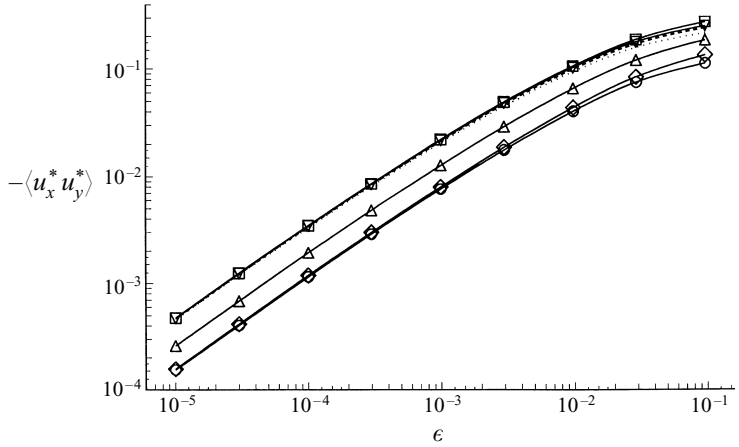

FIGURE 8. The moment of the velocity distribution $-\langle u_x^* u_y^* \rangle$ as a function of ϵ. ○, $e_t = e_n = 0.3, e = 1.0$; △, $e_t = e_n = 0.5, e = 1.0$; □, $e_t = e_n = 0.7, e = 1.0$; ◇, $e_t = 0.3, e_n = 0.7, e = 1.0$; ∇, $e_t = 0.3, e_n = 0.7, e = 1.0$; – – – –, $e_t = e_n = 0.7, e = 0.7$; · · · · · ·, $e_t = e_n = 0.7, e = 0.5$.

symbolic computation. In this procedure, the sum of a finite number of terms in the series, usually between 200 and 500, was used for the analysis. The number of terms in the series was chosen so that the addition of 100 terms caused a variation of less than 10^{-8} times the value of the sum. The sums obtained in this manner were analysed over a variation in ϵ over four decades $10^{-6} \leqslant (\epsilon/\sin(\chi)) \leqslant 10^{-2}$ for various values of p, e_n and χ to extract the asymptotic behaviour given in (2.30) to (2.32).

The expressions for the mean-square velocities can be simplified using symmetry considerations. It is only necessary to evaluate the integrals over the angles χ_A and χ_B from 0 to π while evaluating the moments in (2.26). The values of the integrals from π to 2π for χ_A and from $-\pi$ to 0 for χ_B can be obtained using the symmetry of the distribution function. The mean-square velocity in the x-direction obtained in this manner is

$$\langle u_x^{*2} \rangle = 1 + 2 \sum_{I=A,B} \int_0^\pi \mathrm{d}\chi_I f_{I0}(\chi_I) \left[\sum_{i=0}^{\infty} \frac{2(-1)^{(i-1)} e_t^i}{e_n^i} \prod_{j=1}^{i} \left[1 + \frac{2\epsilon}{(e_n)^j |\sin(\chi_I)|} \right]^{-1} \right]$$

$$+2 \sum_{I=A,B} \int_0^\pi \mathrm{d}\chi_I (1 + \cos(\chi_I)^2) f_{I0}(\chi_I) \left[\sum_{i=0}^{\infty} \frac{e_t^{2i}}{e_n^i} \prod_{j=1}^{i} \left[1 + \frac{2\epsilon}{(e_n)^j |\sin(\chi_I)|} \right]^{-1} \right]. \quad (2.33)$$

In addition, a further simplification is possible because the values of the integrals for the particles of type A and B are equal. In (2.33), $f_{I0}(\chi_I)$ is proportional to ϵ when u_x^* is $O(1)$ different from $\pm V$, and $(\langle u_x^{*2} \rangle - 1)$ is proportional to $\epsilon^{1-\alpha}$ for $e_t^2 > e_n$, and proportional to ϵ for $e_t^2 < e_n$ in the limit $\epsilon \to 0$ (from (2.32)).

The mean-square velocity $\langle u_y^{*2} \rangle$ is

$$\langle u_y^{*2} \rangle = \sum_{I=A,B} \sum_{i=0}^{\infty} \int_0^\pi \mathrm{d}\chi_I f_{Ii}(\chi_I) [e_n^i \sin(\chi_I)]^2$$

$$= \sum_{I=A,B} \int_0^\pi \mathrm{d}\chi_I \sin(\chi_I)^2 f_{I0}(\chi_I) \left[\sum_{i=0}^{\infty} e_n^i \prod_{j=1}^{i} \left[1 + \frac{2\epsilon}{(e_n)^j |\sin(\chi_I)|} \right]^{-1} \right]. \quad (2.34)$$

For $u_y^* \sim 1$, $f_{I0}(\chi_I)$ is proportional to ϵ in the limit $\epsilon \to 0$ and the term in the square brackets converges to a constant (from (2.31)). Near the points $(\pm V, 0)$ where $f_{I0} = O(1)$, the velocity $u_y^* \sim \epsilon^{1/2}$, and therefore $\langle u_y^{*2} \rangle$ has the behaviour given in (2.28). The correlation $\langle u_x^* u_y^* \rangle$ is

$$
\begin{aligned}
-\langle u_x^* u_y^* \rangle &= \sum_{I=A,B} \sum_{i=0}^{\infty} \int \mathrm{d}\chi_I f_{Ii}(\chi_I) e_n^i \sin(\chi_I)(1 + (-1)^{(i-1)} e_t^i - e_t^i \cos(\chi_I)) \\
&= \sum_{I=A,B} \int \mathrm{d}\chi_I \sin(\chi_I) f_{I0}(\chi_I) \left[\sum_{i=0}^{\infty} (1 + (-1)^{(i-1)} e_t^i - e_t^i \cos(\chi_I)) \right. \\
&\quad \left. \times \prod_{j=1}^{i} \left[1 + \frac{2\epsilon}{(e_n)^j |\sin(\chi_I)|} \right]^{-1} \right]. \qquad (2.35)
\end{aligned}
$$

Using (2.30) and arguments similar to those used above it can easily be seen that $-\langle u_x^* u_y^* \rangle \sim -\epsilon \log(\epsilon)$ in the limit $\epsilon \to 0$ as given in (2.29).

The shear and normal stresses at the wall can be derived using the expressions for the moments of the velocity distribution function. The normal stress at the wall at $y = L/2$ due to collision of particles with velocity $u_y > 0$ is

$$
\tau_{yy} = \sum_{I=A,B} \int_0^{\pi} \mathrm{d}\chi_I \left(\sum_{i=0}^{\infty} f_{Ii}(\chi_I)(n u_{Iy}^{(i)})[(1 + e_n) m u_{Iy}^{(i)}] \right), \qquad (2.36)
$$

where the term $n u_{Iy}^{(i)}$ is the frequency of collision per unit length with the wall at $y = L/2$, $(1 + e_n) m u_{Iy}^{(i)}$ represents the impulse transmitted to the wall during a collision and is the negative of the change in the momentum of the particle during a collision. Here m is the mass of the particle. In (2.36), the angle χ_I has been integrated between 0 and π since the velocity $u_{Iy}^{(i)}$ has to be positive for a collision with the wall at $y = L/2$. The expression can easily be simplified to yield

$$
\tau_{yy} = nmV^2 (1 + e_n) \tfrac{1}{2} \langle u_y^{*2} \rangle. \qquad (2.37)
$$

From the above equation, it can be inferred that $\tau_{yy} \sim \epsilon$ in the limit $\epsilon \to 0$. The shear stress at the wall at $y = L/2$ due to collisions of particles with $u_y > 0$ is

$$
\tau_{xy} = \sum_{I=A,B} \int_0^{\pi} \mathrm{d}\chi_I \left(\sum_{i=0}^{\infty} f_{Ii}(\chi_I)(n u_{Iy}^{(i)})[(1 - e_t) m (V_w - u_{Ix}^{(i)})] \right), \qquad (2.38)
$$

where the impulse transmitted to the wall, $(1 - e_t) m (V_w - u_{Ix}^{(i)})$, is the negative of the change in the particle momentum during the collision. The above expression can be reduced to

$$
\tau_{xy} = nm(1 - e_t)[V V_w \langle u_y^* \rangle_* - V^2 \tfrac{1}{2} \langle u_x^* u_y^* \rangle], \qquad (2.39)
$$

where

$$
\langle u_y^* \rangle_* = \sum_{I=A,B} \int_0^{\pi} \mathrm{d}\chi_I \sum_{i=0}^{\infty} f_{Ii}(\chi_I) u_{Iy}^{(i)}. \qquad (2.40)
$$

Using (2.30), it can easily be verified that

$$
\lim_{\epsilon \to 0} [\langle u_y^* \rangle_*] \sim -\epsilon \log(\epsilon), \qquad (2.41)
$$

and the shear stress τ_{xy} is proportional to $-\epsilon \log(\epsilon)$ in this limit.

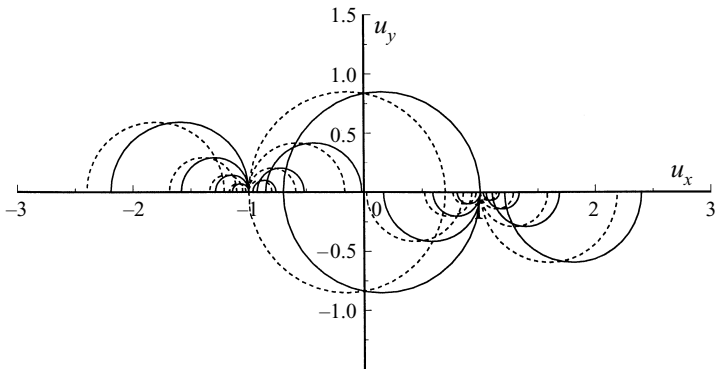

FIGURE 9. The contours C_i of the particle velocities in the (u_x, u_y)-plane for particles undergoing inelastic binary collisions. The solid lines show the location of particles whose velocity before the binary collision is $(+V, 0)$, while the broken lines show the location of the particles whose velocity before the binary collision is $(-V, 0)$. The coefficient of restitution of wall collisions, e_t and e_n, and the coefficient of restitution of binary collisions, e, are all 0.7.

The effect of inelastic binary collisions between particles is considered next. As before, the system consists of particles of diameter a and number density n in a channel of width L, and the coefficients of restitution of particle–wall collisions are e_t and e_n in the directions normal and tangential to the wall. However, the binary collisions are considered to be inelastic with a coefficient of restitution e. Consider a collision between particle A with velocity $(u_{Ax}, u_{Ay}) = (V, 0)$ and particle B with velocity $(u_{Bx}, u_{By}) = (-V, 0)$ as shown in figure 1. The velocities of the particles after collision, analogous to (2.6), are

$$\left.\begin{aligned} u'_{Ax} &= V\,[e_- - e_+ \cos(2\theta)]\,, \qquad u_{Ay} = -Ve_+ \sin(2\theta), \\ u'_{Bx} &= V\,[-e_- + e_+ \cos(2\theta)]\,, \quad u_{By} = Ve_+ \sin(2\theta), \end{aligned}\right\} \tag{2.42}$$

where $e_+ = (1+e)/2$ and $e_- = (1-e)/2$. The particle A with a precollisional velocity $(V, 0)$ is displaced onto a circle in velocity space centred at (Ve_-) with radius (Ve_+), while the particle B with a precollisional velocity $(-V, 0)$ is displaced onto a circle centred at $(-Ve_-)$ with the same radius (Ve_+) as shown in figure 9. As before, the velocity distribution is determined using the polar coordinates, (u_A, χ_A) and (u_B, χ_B). These are related to the angle θ by

$$\left.\begin{aligned} u_A &= Ve_+, \quad \chi_A = \pi + 2\theta, \\ u_B &= Ve_+, \quad \chi_B = 2\theta, \end{aligned}\right\} \tag{2.43}$$

where θ varies between $-\pi/2$ and $\pi/2$, χ_A varies between 0 and 2π and χ_B varies between $-\pi$ and π.

The distribution functions are evaluated in a manner similar to the derivation for a system with elastic binary collisions. The distribution functions $f_{A0}(\chi_A)$ and $f_{B0}(\chi_B)$, analogous to (2.13), are

$$\left.\begin{aligned} f_{A0}(\chi_A) &= \frac{\epsilon}{4(e_+|\sin(\chi_A)| + 2\epsilon)} \left[\cos\left(\tfrac{1}{2}\chi_A - \tfrac{1}{2}\pi\right)\right], \\ f_{B0}(\chi_B) &= \frac{\epsilon}{4(e_+|\sin(\chi_B)| + 2\epsilon)} \left[\cos\left(\tfrac{1}{2}\chi_B\right)\right]. \end{aligned}\right\} \tag{2.44}$$

The dispersion of the particle velocities due to subsequent wall collisions is very

similar to that analysed earlier for elastic binary collisions. The velocity components of a particle which has undergone i collisions with the wall after the most recent binary collision, analogous to (2.14), are

$$\left.\begin{aligned} u_{Ax}^{(i)} + (1+(-1)^{(i-1)}e_t^i)V &= e_t^i V(e_+\cos(\chi_A)+e_-) \quad \text{for} \quad 0<\chi_A<\pi, \\ u_{Ax}^{(i)} - (1+(-1)^{(i-1)}e_t^i)V &= e_t^i V(e_+\cos(\chi_A)+e_-) \quad \text{for} \quad \pi<\chi_A<2\pi, \\ u_{Ay}^{(i)} &= e_n^i e_+ V\sin(\chi_A), \end{aligned}\right\} \tag{2.45}$$

$$\left.\begin{aligned} u_{Bx}^{(i)} + (1+(-1)^{(i-1)}e_t^i)V &= e_t^i V(e_+\cos(\chi_B)-e_-) \quad \text{for} \quad 0<\chi_B<\pi, \\ u_{Bx}^{(i)} - (1+(-1)^{(i-1)}e_t^i)V &= e_t^i V(e_+\cos(\chi_B)-e_-) \quad \text{for} \quad -\pi<\chi_B<0, \\ u_{By}^{(i)} &= e_n^i e_+ V\sin(\chi_B), \end{aligned}\right\} \tag{2.46}$$

and the corresponding distribution functions are

$$f_{Ai} = \frac{f_{A0}}{e_n^i}\prod_{j=1}^{i}\left[1+\frac{2\epsilon}{e_n^j e_+|\sin(\chi_A)|}\right], \quad f_{Bi} = \frac{f_{B0}}{e_n^i}\prod_{j=1}^{i}\left[1+\frac{2\epsilon}{e_n^j e_+|\sin(\chi_B)|}\right]. \tag{2.47}$$

It can easily be verified that the above distribution functions are also normalized, and the moments of the velocity distribution function can be evaluated in a manner similar to that for the case of elastic binary collisions. The moments of the distribution function for a system of disks with inelastic binary collisions are shown in figures 6, 7 and 8. The particle–wall coefficients of restitution are $e_t = e_n = 0.7$, while the coefficient of restitution for the binary collisions is $e = 0.7$ (broken line) and $e = 0.5$ (dotted line). It can be seen that the effect of inelastic binary collisions only leads to a quantitative change in the moments of the velocity distribution, while the scaling laws in the limit $\epsilon \to 0$ remain unchanged.

3. Inelastic spheres in three dimensions

The extension of the above analysis to a three-dimensional system is briefly discussed in this section. The coordinate axes x and y are chosen parallel and perpendicular to the walls of the channel in the plane of shear, while the z-axis is perpendicular to the plane of shear. The frequency of wall collisions per unit volume in the present case is nu_y/L, where n is now the number of particles per unit volume, while the frequency of binary collisions is proportional to $n^2\pi a^2 V$, where V is the magnitude of the particle velocities. In the limit where the frequency of wall collisions is large compared to that of binary collisions, the small parameter $\epsilon = na^2L$ is used for the asymptotic analysis.

As in the two-dimensional case, the particle velocities approach $(\pm V, 0, 0)$ after successive collisions with the walls, where $V = (1-e_t)V_w/(1+e_t)$. The evolution of the velocity of a particle with initial velocity (u_{x0}, u_{y0}, u_{z0}) due to successive wall collisions is

$$u_x + (-1)^i(1+(-1)^{i-1}e_t^i)V = e_t^i u_{x0}, \quad u_y = (-1)^i e_n^i u_{y0}, \quad u_z = e_t^i u_{z0}, \tag{3.1}$$

where i denotes the number of collisions with the wall after the most recent binary collision, and it is assumed that the first collision takes place with the wall at $y = L/2$.

The effect of binary collisions is analysed in a manner similar to that for inelastic disks in two dimensions. In the leading approximation, only collisions between particle A with velocity $(V, 0, 0)$ and particle B with velocity $(-V, 0, 0)$ are considered, since

most of the particles have velocities close to $(\pm V, 0, 0)$ in the limit $\epsilon \to 0$. The result of the collision depends on the azimuthal and meridional angles made by the line joining the centres of the particles with the x-axis, θ and ϕ. Here, θ is the angle made by the line joining the centres with the x-axis, while ϕ is the angle made by the projection of the line of centres on the (y,z)-plane with the y-axis. The components of the velocity after the collision are

$$\left.\begin{aligned} u'_{Ax} &= -V\cos(2\theta), \quad u'_{Ay} = -V\sin(2\theta)\cos(\phi), \quad u'_{Az} = -V\sin(2\theta)\sin(\phi), \\ u'_{Bx} &= V\cos(2\theta), \quad\quad u'_{By} = V\sin(2\theta)\cos(\phi), \quad\quad u'_{Bz} = V\sin(2\theta)\sin(\phi), \end{aligned}\right\} \tag{3.2}$$

where the subscripts A and B refer to particles whose precollisional velocities in the x-direction are positive and negative respectively. The components of the velocity after the collision, expressed in spherical polar coordinates, are

$$\left.\begin{aligned} u_A &= V, \quad \chi_A = \pi - 2\theta, \quad \eta_A = \pi + \phi, \\ u_B &= V, \quad \chi_B = 2\theta, \quad\quad \eta_B = \phi. \end{aligned}\right\} \tag{3.3}$$

The ranges of the azimuthal and meridional angles are $0 \leqslant \chi_A \leqslant \pi$, $0 \leqslant \chi_B \leqslant \pi$, $\pi \leqslant \eta_A \leqslant 3\pi$ and $0 \leqslant \eta_B \leqslant 2\pi$. The particles are displaced onto a sphere of radius V centred at the origin in velocity space. The frequency of binary collisions per unit volume for which the azimuthal and meridional angles are in the range $(\mathrm{d}\theta, \mathrm{d}\phi)$ about (θ, ϕ) is

$$\text{Frequency/Volume} = (n/2)^2(2V)a\cos(\theta)\sin(\theta)\mathrm{d}\theta\mathrm{d}\phi. \tag{3.4}$$

Using (3.3), the collisional influx of particles in the differential solid angle $(\mathrm{d}\chi_I, \mathrm{d}\eta_I)$ about (χ_I, η_I) on the sphere of radius V is

$$\left.\begin{aligned} N_A^{in}(\chi_A,\eta_A)\mathrm{d}\chi_A\mathrm{d}\eta_A &= \tfrac{1}{4}n^2Va\left[\cos\left(\tfrac{1}{2}\pi - \tfrac{1}{2}\chi_A\right)\sin\left(\tfrac{1}{2}\pi - \tfrac{1}{2}\chi_A\right)\right]\mathrm{d}\chi_A\mathrm{d}\eta_A, \\ N_B^{in}(\chi_B,\eta_B)\mathrm{d}\chi_A\mathrm{d}\eta_A &= \tfrac{1}{4}n^2Va\left[\cos\left(\tfrac{1}{2}\chi_B\right)\sin\left(\tfrac{1}{2}\chi_B\right)\right]\mathrm{d}\chi_B\mathrm{d}\eta_B. \end{aligned}\right\} \tag{3.5}$$

The flux of particles out of the sphere of radius V due to wall collisions and binary collisions is

$$N_I^{out}(\chi_I,\eta_I) = (n|u_{Iy}|/L + n^2\pi a^2 V)f_{I0}(\chi_I,\eta_I) \tag{3.6}$$

for $I = A, B$, where f_{I0} is the distribution function, and $nf_{I0}(\chi_I,\eta_I)\mathrm{d}\chi_I\mathrm{d}\eta_I$ is the number of particles per unit volume in the differential angle $(d\chi_I, d\eta_I)$ about (χ_I, η_I) on the sphere of radius V in velocity space. The assumptions made while deriving (3.6) are identical to those made while deriving (2.12) for a two-dimensional case. At steady state, $N_I^{in}(\chi_I,\eta_I) = N_I^{out}(\chi_I,\eta_I)$ and the distribution function f_{I0} is

$$\left.\begin{aligned} f_{A0}(\chi_A,\eta_A) &= \frac{\epsilon}{4(|\sin(\chi_A)\cos(\eta_A)} + \pi\epsilon)\left[\cos\left(\tfrac{1}{2}\pi - \tfrac{1}{2}\chi_A\right)\sin\left(\tfrac{1}{2}\pi - \tfrac{1}{2}\chi_A\right)\right], \\ f_{B0}(\chi_B,\eta_B) &= \frac{\epsilon}{4(|\sin(\chi_B)\cos(\eta_B)} + \pi\epsilon)\left[\cos\left(\tfrac{1}{2}\chi_B\right)\sin\left(\tfrac{1}{2}\chi_B\right)\right]. \end{aligned}\right\} \tag{3.7}$$

Subsequent wall collisions alter the particle velocities, and the velocity of the particle after i collisions with the walls following the most recent binary collision is

$$\left.\begin{aligned} u_{Ix}^{(i)} + (1 + (-1)^{(i-1)}e_t^i)V &= e_t^i V\cos(\chi_I) \quad \text{for} \quad -\pi/2 < \phi < \pi/2, \\ u_{Ix}^{(i)} - (1 + (-1)^{(i-1)}e_t^i)V &= e_t^i V\cos(\chi_I) \quad \text{for} \quad \pi/2 < \phi < 3\pi/2, \\ u_{Iy}^{(i)} &= e_n^i V\sin(\chi_I)\cos(\eta_I), \\ u_{Iz}^{(i)} &= e_t^i V\sin(\chi_I)\sin(\eta_I). \end{aligned}\right\} \tag{3.8}$$

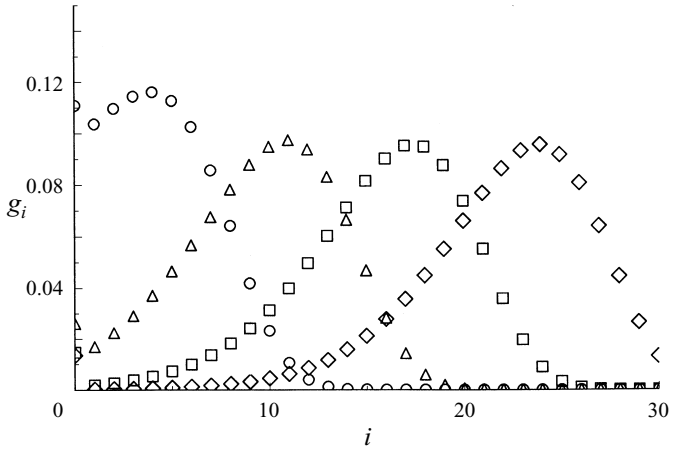

FIGURE 10. The number of particles g_i on contour C_i as a function i for a three-dimensional system. The coefficients of restitution e_t and e_n are both 0.7. ○, $\epsilon = 10^{-2}$; △, $\epsilon = 10^{-3}$; □, $\epsilon = 10^{-4}$; ◇, $\epsilon = 10^{-5}$.

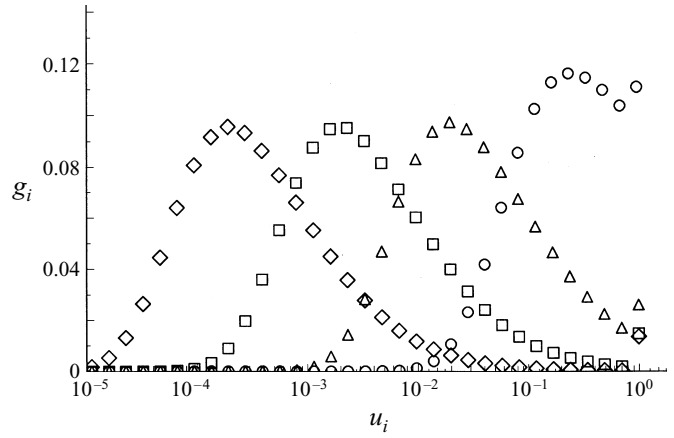

FIGURE 11. The number of particles g_i on contour C_i as a function u_i, the radius of contour C_i for a three-dimensional system. The coefficients of restitution e_t and e_n are both 0.7. ○, $\epsilon = 10^{-2}$; △, $\epsilon = 10^{-3}$; □, $\epsilon = 10^{-4}$; ◇, $\epsilon = 10^{-5}$.

The particle positions are located on ellipsoids of revolution S_i centred about $(\pm(1 + e_t^i)V, 0, 0)$ with radii $e_t^i V$ along the x- and z-directions and $e_n^i V$ along the y-direction. The intersection of the ellipsoids with the (x, y)-plane is identical to the contours C_i shown in figure 2. The accumulation and depletion of particles on the i^{th} surface, analogous to (2.15) and (2.17) are

$$N_{Ii}^{in}(\chi_I, \eta_I) = (n|u_{Iy}^{(i-1)}|/L) f_{I(i-1)}(\chi_I), \tag{3.9}$$

$$N_{Ii}^{out}(\chi_I, \eta_I) = [(n|u_{Iy}^{(i)}|/L) + \pi n^2 a V] f_{Ii}(\chi_I). \tag{3.10}$$

Equating $N_{Ii}^{in}(\chi_I, \eta_I)$ and $N_{Ii}^{out}(\chi_I, \eta_I)$ at steady state, the distribution function is

$$f_{Ii}(\chi_I, \eta_I) = \frac{f_{I(i-1)}(\chi_I, \eta_I)}{e_n} \left[1 + \frac{\pi \epsilon V}{|u_{Iy}^{(i)}|}\right]^{-1}. \tag{3.11}$$

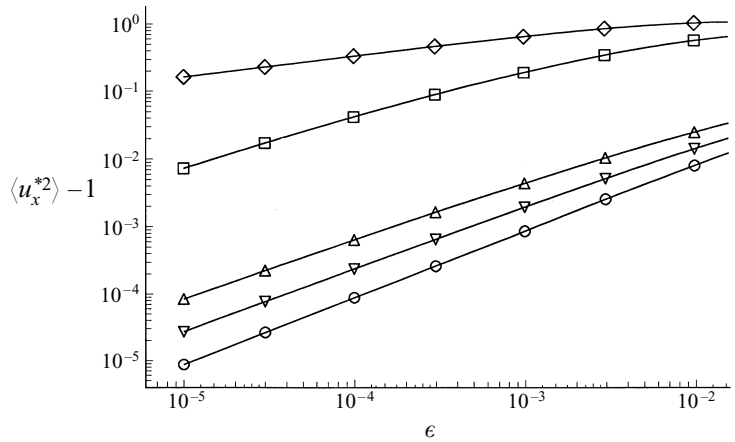

FIGURE 12. The mean-square velocity $\langle u_x^{*2}\rangle - 1$ as a function of ϵ for a three-dimensional system and elastic binary collisions. ◯, $e_t = e_n = 0.3$; △, $e_t = e_n = 0.5$; □, $e_t = e_n = 0.7$; ◇, $e_t = 0.7, e_n = 0.3$; ∇, $e_t = 0.3, e_n = 0.7$.

Finally, the distribution function can be expressed in terms of $f_{I0}(\chi_I, \eta_I)$ using induction:

$$f_{Ii}(\chi_I, \eta_I) = \frac{f_{I0}(\chi_I, \eta_I)}{e_n^i} \prod_{j=1}^{i} \left[1 + \frac{\pi\epsilon}{e_n^j |\sin(\chi_I)\cos(\eta_I)|}\right]. \tag{3.12}$$

As in the case of inelastic disks in two dimensions, it can easily be verified that the above distribution function is normalized:

$$\sum_{I=A,B} \sum_{i=0}^{\infty} \int \mathrm{d}\eta_I \int_0^{\pi} \mathrm{d}\chi_I \sin(\chi_I) f_{Ii}(\chi_I, \eta_I) = 1, \tag{3.13}$$

where the range of integration is $\pi \leqslant \eta_A \leqslant 3\pi$ and $0 \leqslant \eta_B \leqslant 2\pi$.

The fraction of the particles on the surface S_i in velocity space, g_i, is

$$g_i = \sum_{I=A,B} \int \mathrm{d}\eta_I \int_0^{\pi} \mathrm{d}\chi_I \sin(\chi_I) f_{Ii}(\chi_I, \eta_I), \tag{3.14}$$

where the limits of integration for the angle η_I are $\pi \leqslant \eta_I \leqslant 3\pi$ for $I = A$ and $0 \leqslant \eta_I \leqslant 2\pi$ for $I = B$. The fraction g_i is shown as a function of i in figure 10, and as a function of $u_i = e_n^i$ in figure 11. Figure 11 shows that the velocities of the particles are close to $(\pm V, 0, 0)$ only for $\epsilon \leqslant 10^{-3}$, in contrast to the two-dimensional case (figure 4) where the equivalent condition was $\epsilon \leqslant 10^{-2}$. Therefore, the assumptions made while deriving the distribution function for the three-dimensional geometry are valid over a smaller range of ϵ than those for the two-dimensional case. The qualitative reason for this is as follows. In the two-dimensional geometry, the binary collisions scatter particles onto a circle in velocity space, and these particles subsequently approach $(\pm V, 0, 0)$ due to repeated collisions. The collision frequency of these particles is proportional to u_y, which is non-zero at all points on the circle C_0 except near $(\pm V, 0)$. In the three-dimensional case, the particles are scattered onto a surface S_0 in velocity space, and the depletion of particles due to wall collisions is proportional to u_y. Therefore, the particles on the contour that is the intersection of the surface S_0 with the (u_x, u_z)-plane do not experience wall collisions, and the depletion of these particles is due to binary collisions alone. Due to this, the assumption that the

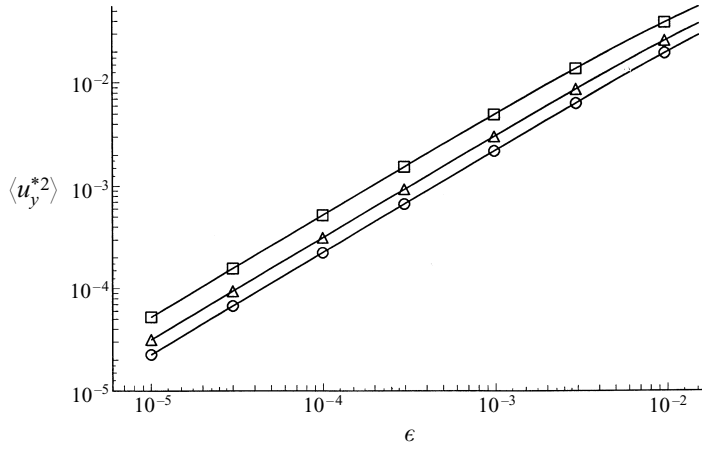

FIGURE 13. The mean-square velocity $\langle u_y^{*2} \rangle$ as a function of ϵ for a three-dimensional system and elastic binary collisions. ◯, $e_t = e_n = 0.3$; △, $e_t = e_n = 0.5$; □, $e_t = e_n = 0.7$.

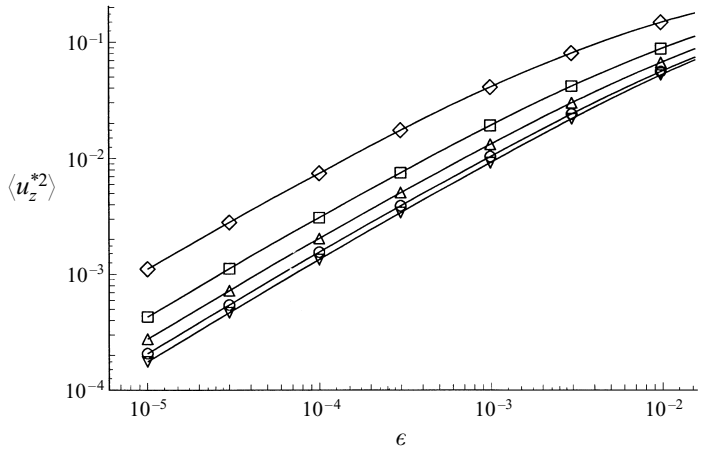

FIGURE 14. The mean-square velocity $\langle u_z^{*2} \rangle$ as a function of ϵ for a three-dimensional system and elastic binary collisions. ◯, $e_t = e_n = 0.3$; △, $e_t = e_n = 0.5$; □, $e_t = e_n = 0.7$; ◇, $e_t = 0.7, e_n = 0.3$; ∇, $e_t = 0.3, e_n = 0.7$.

particles have velocities close to $(\pm V, 0, 0)$ is less accurate in the three-dimensional than in the two-dimensional case.

The moments of the velocity distribution, $\langle u_x^{*2} \rangle - 1$, $\langle u_y^{*2} \rangle$, $\langle u_z^{*2} \rangle$ and $-\langle u_x^* u_y^* \rangle$ are shown in figures 12, 13, 14 and 15 respectively. The asymptotic behaviour of these moments is identical to those for the two-dimensional system analysed in §2. In addition, it is seen that $\langle u_z^{*2} \rangle \sim \epsilon$ for $\epsilon \to 0$. The reasons for the limiting behaviour for these moments can be easily deduced using arguments similar to those for a two-dimensional system, and so these are not discussed in detail here. From the above scalings for the moments of the velocity distribution, the asymptotic behaviour of the normal stresses is $\tau_{yy} \sim \epsilon$ and $\tau_{zz} \sim \epsilon$, and the shear stress $\tau_{xy} \sim \epsilon \log(\epsilon)$ in the limit $\epsilon \to 0$.

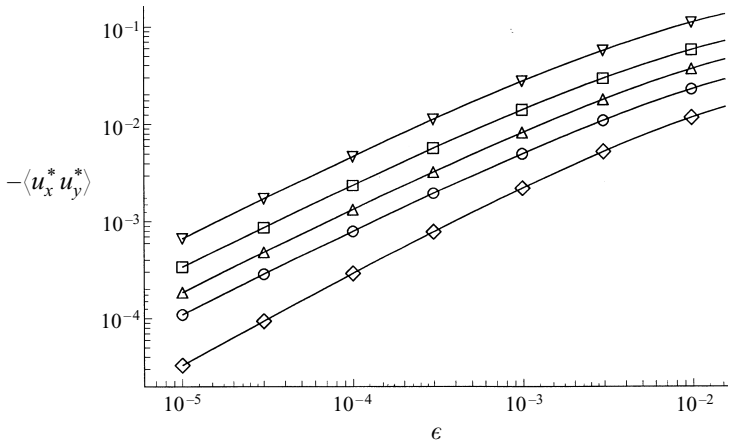

FIGURE 15. The moment of the velocity distribution $-\langle u_x^* u_y^* \rangle$ as a function of ϵ for a three-dimensional system and elastic binary collisions. ◯, $e_t = e_n = 0.3$; △, $e_t = e_n = 0.5$; □, $e_t = e_n = 0.7$; ◇, $e_t = 0.7, e_n = 0.3$; ∇, $e_t = 0.3, e_n = 0.7$.

4. Conclusions

In the present analysis, the velocity distribution function of a granular material in shear flow in a channel was determined in the limit where the frequency of particle–wall collisions is large compared to the frequency of binary collisions between particles. The walls of the channel were separated by a distance L, and were considered to be moving with constant velocities $+V_w$ and $-V_w$. In this regime, an asymptotic analysis was used in the small parameter ϵ, which is equal to naL in two dimensions and naL^2 in three dimensions, where n is the particle number density and a is the particle diameter. The dynamics of particle–wall collisions was described by simple relations (2.1) with constant coefficients of restitution. The present analysis can be extended quite easily for collisions described by a specularity coefficient, where the probability of a particle being reflected with a certain angle is known. However, analysis of this type cannot be easily carried out for the case where the tangential coefficient of restitution depends on the normal velocity. The binary collisions were considered to be elastic in most of the analysis, but the effect of inelastic binary collisions was analysed for the two-dimensional geometry at the end of §2. It was found that inelastic binary collisions did not qualitatively alter the results for the moments of the velocity distribution.

The velocity distribution function at steady state was determined using a self-consistent procedure. First, binary collisions were neglected in the limit $\epsilon \ll 1$, and two fixed points $(\pm V, 0)$ were identified in velocity space to which all particle velocities converge after repeated collisions with the walls. These two fixed points have zero velocity normal to the walls, and equal and opposite velocities in the tangential direction. Collisions between particles at these two points results in a scattering of the particle velocities onto a sphere of radius V in three dimensions or a circle of diameter V in two dimensions. Subsequent wall collisions transport the particles onto certain elliptical contours in velocity space, and the distribution function is zero elsewhere. The distribution function along the elliptical contours were determined using a flux balance at steady state. This calculation is not exact, because the particles were assumed to be at the fixed points $(\pm V, 0)$ while calculating the fluxes due to binary collisions in order to obtain analytical results for the distribution function.

The error made due to this approximation was estimated using the approximate distribution function, and it was found to decrease proportional to $\epsilon^{1/2}$ in the limit $\epsilon \to 0$. The moments of the velocity distribution function were determined, and the scaling relations in the limit $\epsilon \to 0$ were the same for two- and three-dimensional systems. These are summarized in (2.27), (2.28) and (2.29). In addition, it was found that the normal stress is proportional to ϵ and the shear stress is proportional to $\epsilon \log(\epsilon^{-1})$ in the limit $\epsilon \to 0$.

REFERENCES

Cercignani, C. 1975 *The Boltzmann Equation and its Applications*. Springer.

Chapman, S. & Cowling, T. G. 1970 *The Mathematical Theory of Nonuniform Gases*, 3rd Edn. Cambridge University Press.

Foerster, S. F., Louge, M. Y., Chang, H. & Allia, K. 1994 Measurements of collision properties of small spheres. *Phys. Fluids* **6**, 1108–1115.

Jenkins, J. T. 1987 Balance laws and constitutive relations for rapid flows of granular materials. In *Proc. Army Research Office Workshop on Constitutive Relations* (ed. J. Chandra & R. Srivastava), *Philadelphia*.

Jenkins, J. T. 1992 Boundary conditions for rapid granular flows: flat, frictional walls. *Trans. ASME* E: *J. Appl. Mech.* **59**, 120–143.

Jenkins, J. T. & Askari, E. 1991 Boundary conditions for rapid granular flows: plane interfaces. *J. Fluid Mech.* **223**, 497–508.

Jenkins, J. T. & Richman, M. W. 1985 Kinetic theory for plane flows of a dense gas of identical, rough, inelastic circular disks. *Phys. Fluids* **28**, 3485–3494.

Jenkins, J. T. & Richman, M. W. 1986 Boundary conditions for plane flows of smooth, nearly elastic, circular disks. *J. Fluid Mech.* **171**, 53–69.

Jenkins, J. T. & Richman, M. W. 1988 Plane simple shear of smooth inelastic circular disks: the anisotropy of the second moment in dilute and dense limits. *J. Fluid Mech.* **192**, 313–328.

Jenkins, J. T. & Savage, S. B. 1983 A theory for the rapid flow of identical, smooth, nearly elastic spherical particles. *J. Fluid Mech.*, **130**, 187–202.

Johnson, P. C. & Jackson, R. 1987 Frictional– collisional constitutive relations for granular materials, with application to plane shearing. *J. Fluid Mech.* **176**, 67–93.

Kumaran, V. & Koch, D. L. 1993 Properties of a bidisperse gas–solid suspension. Part 2. Viscous relaxation time small compared to collision time. *J. Fluid Mech.* **247**, 643–660.

Kumaran, V., Tsao, H.-K. & Koch, D. L. 1993 Velocity distribution functions for a bidisperse sedimenting particle–gas suspension. *Intl J. Multiphase Flow* **19**, 665–681.

Lun, C. K. K. 1991 Kinetic theory for granular flow of dense, slightly inelastic, slightly rough spheres. *J. Fluid Mech.* **233**, 539–559.

Lun, C. K. K. & Savage, S. B. 1987 A simple kinetic theory for granular flows of rough, inelastic spherical particles. *Trans. ASME* E: *J. Appl. Mech.* **54**, 47–53.

Lun, C. K. K., Savage, S. B., Jeffrey, D. J. & Chepurniy, N. 1984 Kinetic theories for granular flow: inelastic particles in Couette flow and slightly inelastic particles in a general flow fields. *J. Fluid Mech.* **140**, 223–256.

Savage, S. B. 1982 Granular flows down rough inclines - review and extension. In *Proc. US–Japan Seminar on New Models and Constitutive Relations in Mechanics of Granular Materials* (ed. J. T. Jenkins & M. Satake). Elsevier.

Tsao, H.- K. & Koch, D. L. 1995 Simple shear flows of dilute gas–solid suspensions. *J. Fluid Mech.* **296**, 211–245.

Walton, O. R. 1992 Numerical simulations of inelastic, frictional particle–particle interactions. In *Particulate Two–Phase Flow* (ed. M. C. Roco). Butterworth-Heinman.